Experimental Study of Hydraulic Sealability and Shear Bond Strength of Cementitious Barrier Materials

Mohammadreza Kamali[1]
Department of Energy and Petroleum Engineering,
University of Stavanger,
Stavanger 4036, Norway
e-mail: mohammadreza.kamali@uis.no

Mahmoud Khalifeh
Department of Energy and Petroleum Engineering,
University of Stavanger,
Stavanger 4036, Norway
e-mail: mahmoud.khalifeh@uis.no

Elsayed Eid
Department of Energy and Petroleum Engineering,
University of Stavanger,
Stavanger 4036, Norway
e-mail: e.eid@stud.uis.no

Arild Saasen
Department of Energy and Petroleum Engineering,
University of Stavanger,
Stavanger 4036, Norway
e-mail: arild.saasen@uis.no

In this experimental study, two different cementitious materials, including (i) a class of expansive cement currently used for plug and abandonment (P&A) operations and (ii) a non-cement-based naturally occurring rock, known as geopolymer, are selected to examine the hydraulic bond strength and shear bond strength. Clean machined steel and rusty corroded steel were selected to represent the casing. The test samples were cured at 90 °C considered as bottom-hole static temperature (BHST) and under elevated pressure of 17.2 MPa for 1 week. The hydraulic sealability of the barrier materials tested up to 3.4 MPa of differential pressure. The results indicated that additives used in slurry preparation impact the hydraulic sealability of the material. Additionally, the rusty corroded steel provided a better hydraulic sealability comparing to the clean machined steel for the same cementitious material. The shear bond strength test was performed by running the push-out test. According to the present test observations, no correlation was found between the shear bond and hydraulic bond strength of different barrier materials. The geopolymer showed the lowest shear bond strength, while it provided the highest hydraulic sealability.
[DOI: 10.1115/1.4051269]

Keywords: petroleum engineering, cementing operations, petroleum wells-drilling/production/construction

1 Introduction

In drilling operation and well construction, a cementitious slurry is pumped into the wellbore and placed behind the casing. The slurry is solidified and acts as a barrier to seal the annular space between the casing and formation and provide zonal isolation. The barrier material facilitates well construction and production by preventing formation fluid migration between different strata, holding the casing in place, and protecting it from corrosion. Consequently, the cementitious barrier material must be impermeable and be able to make a sufficient bonding to the casing to achieve integrated hydraulic sealability [1].

Ordinary Portland cement (OPC) is the leading material for primary cementing and plug and abandonment (P&A) operations. The chemistry of OPC is well-documented for both operating engineers and scientists, and the material is commercially available. Various chemical additives are introduced to the cement system to improve its performance at downhole conditions [2]. However, OPC is found to have shortcomings after setting including, but not limited to thermal instability, retrogression of mechanical properties due to contamination by drilling mud, low ductility, and shrinkage. Shrinkage of the cement bulk due to the hydration reaction can increase the risk of micro-path formation at the cement–casing and cement-formation interfaces. Besides, poor mud removal, improper cement placement due to eccentricity of casing and wellbore geometry, and gas channeling in the cement sheath can have a detrimental effect on zonal isolation and accelerate well integrity failure. Moreover, the cyclic change in pressure and temperature over the lifespan of the well implies a lot of compaction and tension of the cementitious barrier materials. Such condition requires sufficient flexible cement system with high tensile strength to Young's modulus and compressive strength to Young's modulus ratios. The OPC-based system is brittle in nature and may show a weak performance at downhole condition by forming radial cracks when it is subjected to an excessive load [3–5]. Therefore, researchers and technology providers continuously attempt to improve the quality of set cement and the cementing operation by either new cementing techniques or introducing alternative cementitious materials for the situations that OPC has limitations [6,7].

In zonal isolation and well abandonment operation, shear bond and hydraulic bond strength are two parameters, which contribute to effective hydraulic sealability at the interface of zonal isolation material and its adjacent medium [8]. The shear bond strength represents how strong the bonding is to prevent the movement of casing/cement sheath in the wellbore, and it is quantified as the minimum required force to move the casing within the cement sheath or the cement sheath within the formation. The hydraulic bond strength is the maximum hydraulic force induced by the formation fluid to initiate debonding at the interface. This parameter can be determined by continues pumping fluid at the boundaries until the leakage occurs. The shear bond strength and the hydraulic bond strength at the interface of barrier material and casing are discussed and reviewed in detail in Sec. 1.1. Figure 1 shows a schematic of the wellbore, including formation, casing, and the cement sheath.

1.1 Shear Bond and Hydraulic Bond Strengths.

The shear bond strength effectively resists shear displacement and is expressed as the minimum required force to initiate movement at the interface of two materials, and it is an important indication of the cement ability to support casing string in wellbore [9] mechanically. On the laboratory scale, the shear bond strength between the cementitious material and casing pipe or formation is measured by placing the casing pipe (or a rod with few centimeters in diameter) inside the zonal isolation material or curing the zonal isolation

[1]Corresponding author.

Contributed by the Petroleum Division of ASME for publication in the JOURNAL OF ENERGY RESOURCES TECHNOLOGY. Manuscript received March 17, 2021; final manuscript received May 16, 2021; published online June 7, 2021. Assoc. Editor: Saeed Salehi.

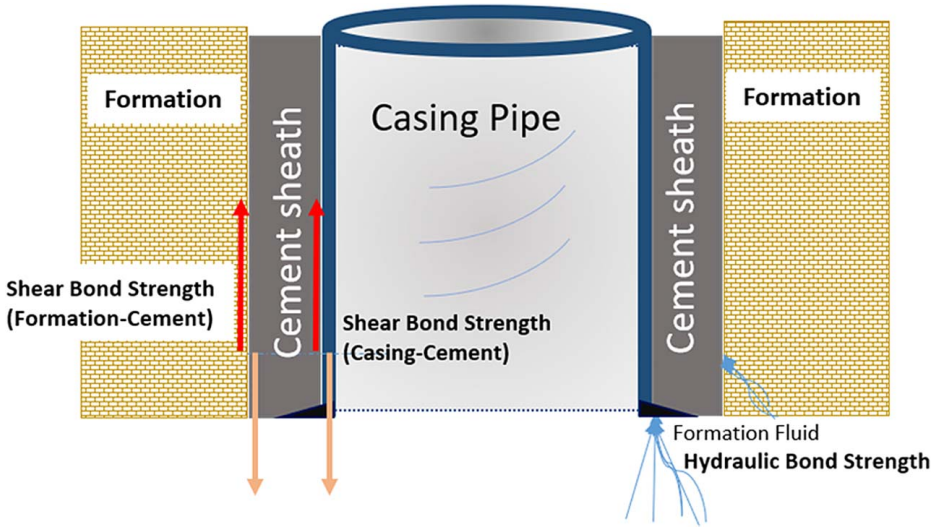

Fig. 1 Schematic of the wellbore including the formation, casing, and the cement sheath. The shear and hydraulic bond strengths are illustrated at the cement–casing and cement-formation interface.

material inside the formation outcrop. Then, a loading frame applies an axial load until debonding occurs, and the inner material starts to slip. One of the early shear bond strength experimental studies was performed by Evans and Carter [10]. The shear bond of different cement systems was investigated with casing and two types of formation, including sandstone and limestone. They reported the shear bond strength between 0.07 and about 2.76 MPa. They stated that shear bond strength depends on curing conditions, including but not limited to curing pressure and temperature, casing surface roughness, drilling fluid existence, and size of specimens. Kakumoto et al. [11] studied the effect of confining pressure on push-out test samples. They applied effective confining pressure of 1.5 and 3 MPa and compared the results with the ambient effective pressure of 0 MPa. The test result shows that increasing the confining pressure around the testing specimens contributes to escalated shear bond strength, depending on the pipe roughness. The authors also showed when the samples reach a maximum load (i.e., maximum load before debonding occurs), the applied load can enter a fluctuation zone. They revealed that it is the effect of stick-slip at the interface of the samples.

Lavrov et al. [12] investigated the effect of casing size on the shear bond strength. The authors studied 37 testing samples with pipe outer diameter (OD) of 10, 21, and 33 mm and height of 30 mm. The samples were cured at 80 °C and under elevated pressure. The tests were performed at displacement control mode with a rate of 0.5 mm/min. The test result shows the same oscillation behavior for the samples caused due to the selected mode of testing. They experimentally proved that the shear bond strength declines by about 36% with an increase in pipe diameter for the selected range of 10–33 mm. One of the limitations of running laboratory experiments is downscaling the real condition to the smaller size, particularly when the materials will go under mechanical loads. One important observation on Lavrov et al.'s test results is the large standard deviation from the mean values of the shear bond strength, which might be due to the small size of the tested samples or inconsistency in the sample preparation. They claimed that bonding strength is not an intrinsic parameter of cement–casing systems and should not be applied to field conditions directly. Using finite-element simulations, they concluded that the normal stress caused by cement shrinkage is reduced at the interface of larger diameters, and it results in less friction resistance of casing and cement. Thus, less push-out strength. In an earlier study conducted by Lavrov et al. [13], they attempted to measure the tensile bond strength between cement and steel using a three-point bending test. They prepared bi-material beams with the dimension of $60 \times 5 \times 5$ cm—$30 \times 5 \times 5$ cm cement and $30 \times 5 \times 5$ cm steel—and cured the specimens for 1 month at ambient pressure and temperature. The samples, however, were not able to be retrieved for testing as all samples were broke at the interface of steel–cement. Hence, they concluded that the push-out test represents friction and mechanical interlock between casing and cement, rather than providing information about adhesion between two materials [12].

In another experimental study, Khalifeh et al. [14] investigated the bond strength of Portland cement with six different pipe materials, including steel (reference material), titanium, two different grades of uncoated aluminum, and two different types of nano-coated aluminum pipes. They prepared the test specimens by curing cement around 50 mm pipes at an elevated temperature of 70 °C and atmospheric pressure for 7 days. The test results revealed that uncoated aluminum pipes provided poor shear bond strength, which is rooted in the detrimental reaction at the interface of the cement–aluminum. On the other hand, the titanium pipes were found to have stronger shear bond strength with Portland cement by 5% greater compared with the cement–steel system. The nano-coated aluminum pipes showed strong shear bond strength compared with the uncoated aluminum pipes. Even, the strength was 13% higher than the cement–steel system. Their study highlighted the possible chemical interaction between cement and the different casing materials.

The characterization of bond strength of geopolymers was studied by Zhang et al. [15] at ambient and elevated temperatures. Their research study included 18 different combinations of metakaolin and fly ash as a solid phase. They tested the shear bond strength in the temperature range of 20–300 °C and concluded that increasing temperature has an adverse effect on the bond strength of geopolymers. The test results also indicated that the chemical composition such as Si/Al ratio, SiO_2/K_2O ratio, and solid/liquid ratio of alkali-activated material significantly impact bond strength. In another study about the characterization of geopolymers for oil and gas applications, Salehi et al. [16] investigated the shear bond strength of class F fly ash geopolymers. In this study, sodium hydroxide (NaOH) with the concentration of 8 M, 10 M, and 12 M was used as a hardener. The experiments were performed at 65 and 93 °C, and the results showed that for mentioned specific fly ash-based system, there is an optimum value for the sodium hydroxide concentration. The maximum bond strength was achieved with 10 M NaOH. It was concluded that an increase in the concentration up to 10 M of alkali hydroxide hardener

accelerates the polymer gel formation, which is responsible for bond strength and compressive strength of geopolymers. Increasing the concentration beyond 10 M for this system affects gel formation and strength development of the slurry and resulting in weaker bonding between the geopolymer and the casing metal. Comparing the test results of fly ash geopolymers with the API class H Portland cement shows slightly higher bond strength for the geopolymers. The researchers highlighted a parameter "fracture energy" accountant for shear bond strength of considered materials. Fracture energy is described as the ability of materials with crack to resist fracture. In this study, this parameter was higher for the geopolymer than the class H cement. In another study about alternative materials for OPC in the oil and gas industry, Khalifeh et al. [17] tested the shear bond strength of a rock-based geopolymer. They used potassium silicate solution as a hardener with SiO_2/K_2O of 2.28 and cured the samples at 70 °C for 7 days. The measured shear bond strength was about 1.3 MPa, which is 3.6% less than the class G cement tested at the same condition. The authors concluded that the hardener modular ratio (SiO_2/M_2O) affects the bond strength of geopolymers (M is an alkali metal, potassium, or sodium).

The principle of shear bond strength is needed to be thoroughly understood. Shear bond strength at the interface of casing and cement can be the summation of (a) friction at the interface of different materials, (b) mechanical interlock due to surface roughness, (c) inward tension at the surface resulting from cement shrinkage, and (d) bonding as a result of chemical interaction between cementitious material and minerals exist at casing surface. However, the latter is a subject of debate.

It is insufficient to have a strong bonding to achieve proper zonal isolation; a cementitious material can have severe adhesion to the casing material, while pathways exist at the interfaces and formation fluid can easily penetrate through micro-channels. Hence, hydraulic bond strength is more critical in terms of zonal isolation, and it should be further investigated [18].

Hydraulic bond strength characterizes the interface between casing and cement material to resist the hydraulic fluid penetration, and it can be considered as a direct measurement of hydraulic sealability and providing zonal isolation [19]. The hydraulic bond strength is defined as minimum pressure induced by an injection fluid to make debonding or initiating flow at cement–casing/formation interface.

Several experimental studies investigated hydraulic bond strength of cement–casing or cement-formation interface at both small- and large-scale [10,14,20]. The experiments were conducted by continuous injection of gas or liquid at the interfaces, and the pressure development and/or the flowrate during the test were monitored. Chemistry and proper placement of the cementitious barrier material, and the pipe surface properties are critical parameters to have integrated hydraulic sealability. The compatibility of the casing material and the cementitious slurry is a necessity. In an earlier experimental study conducted by Khalifeh et al. [14], incompatibility of aluminum pipe and the API neat class G cement was highlighted. Steel pipes are common materials for casing the borehole. For situations that alternative material is required for cementing operation or a new additive is introduced to the cement slurry, it is inevitable to test the system's compatibility and performance.

The output results of hydraulic bond strength tests are relevant for a qualitative comparison between the casing and cementitious materials for both academia and field engineers. The quantitative information, however, includes the non-negligible scaling effect of the test setup. As discussed in the literature [9,12], the small-scale test results provide no guarantee for the exact observation in the field-scale setup. Nonetheless, studying the hydraulic bond strength requires thorough details about micro-path development, size, structure, and direction at the interfaces from a purely academic point of view. Fluid flow through a degraded cement sheath was studied through the visualization of the micro-annuli employing computational fluid dynamics (CFD) and X-ray computed tomography (CT) [21]. Researchers used pressure- and thermal-cycling to mimic real downhole conditions in drilling operations and visualized the fluid flow through the micro paths with the cement sheath and cement–casing interfaces. They concluded that the flow in the macro annuli is a complex phenomenon as it depends on the size and shape of the flow path and the magnitude of degradation of the cement sheath.

1.2 Cementitious Materials. It is crucial to have integrated bonding at the cement–casing or cement-formation interfaces to achieve proper zonal isolation in the well construction. OPC experiences autogenous shrinkage during solidification [22]. In the hydration reaction, the calcium-rich cement powder consumes the water and forms calcium–silicate–hydrate (C–S–H) groups, which are accountable for strength development. When the reaction proceeds, the unreacted cement particles consume free water within the cement matrix and empty the pores. This phenomenon results in autogenous shrinkage and applies internal tensile stress in solidified cement. For situations that the cement sheath has no access to external humidity, the autogenous shrinkage can be extensive and cause radial cracks. Therefore, in oil and gas applications, particularly when the cement slurry is placed between two casings, a higher water to cement ratio is considered [23].

Expansive agents are one of the additives that can compensate the shrinkage to some extent, where the expanding agent can make crystals or generate gas bubbles during the solidification process [24]. The effectiveness of expansive cement for oil and gas applications increases if the expansion reaction occurs at the right time—when the shrinkage starts. Early expansion reaction would not effectively compensate for the long-term shrinkage. While very late expansion can cause cracks in cement structure, it is essential to engineer the chemical reactivity of expanding agents in cement.

Geopolymers are inorganic materials that are produced by mixing a reactive aluminosilicate species with a liquid hardener and make a slurry with cementitious properties [17,25]. In this class of material, the geopolymerization reaction occurs instead of hydration and forms long-chain molecules in tetrahedral orientation, including aluminate and silicate. The solid phase may include low calcium fly ash, metakaolin, or naturally occurring rock. The liquid phase is an alkali silicate solution (potassium or sodium) with an adjusted modular ratio. The geopolymerization reaction proceeds in three main steps: (a) the aluminosilicate structures are dissolved and the silanol groups (Si–O–H) are created, (b) the single groups are oriented and reconnected to form oligomers as the ion concentration increases in the slurry, and finally, (c) the long-chain structure of aluminosilicates is formed through polycondensation and by connecting oligomers. Although geopolymers are used in the civil industry, the technology is still at the research stage for oil and gas application by engineering the properties based on downhole conditions.

In this research work, an expansive commercial cement used for plug and abandonment operation and a rock-based geopolymer are applied, as zonal isolation material, to study shear bond and hydraulic bond strengths of the casing. This study aims to investigate the performance of a different class of materials at similar operational conditions of pressure and temperature and generate a data set including the test results of neat materials. The neat API class G cement was also selected to make the results reproducible as a non-commercial reference. The common additives may also be different depending on material suppliers all around the world.

2 Material Preparation and Experimental Procedures

2.1 Slurry Preparation and Mixing. For all samples, the slurries were mixed using the raw materials, including solid and liquid phases and additives that were delivered by the industrial service providers. The mixing procedure was followed in accordance with the provided instructions by material suppliers and described in detail in the following. The recipes were designed and suggested based on bottom-hole circulation temperature (BHCT) of 65 °C and bottom-hole static temperature (BHST) of

90 °C, and the pressure of 170 bar. This is the condition for majority of wells in North Sea, and it is recommended by operating companies. The rheological properties and pumpability of materials at BHCT, and mechanical properties of materials after solidification up to 28 days of curing were tested and published [26]. All materials used for hydraulic bond strength tests were mixed using the API high-speed mixer Waring blender. The mixer starts to mix the slurry for 15 s at 4000 rpm and continues mixing for 35 more seconds at 12,000 rpm. The shear bond strength specimens needed a higher volume of cementitious slurry; therefore, the API high-speed mixer was not applicable due to its small capacity. Hobart N50-60 commercial blender was used to mix the slurry for the shear bond strength test. The mix design of each material was upscaled and sheared for 30 min, while the mixer speed was fixed at level 2. The mixing procedure and components for each type of barrier material are described as follows:

Neat class G cement—The solid phase consists of only neat API class G cement manufactured by Dyckerhoff. It was mixed with 44% by weight of cement (BOWC) de-ionized water.

Expansive cement—The solid phase was dry blended class G cement with magnesium oxide as an expansive agent, and it was delivered by the material supplier. Industrial chemicals were added to the de-ionized water and formed the liquid phase. The material supplier recommended additives were to tailor the rheological and mechanical properties of the slurry. The additives included in this study were retarder, fluid-loss controller, defoamer, and cement particle dispersant. Microsilica solution with a mass fraction of 50% in water was recommended by the cement supplier to enhance the performance of the material.

Geopolymer—The slurry was mixed based on an in-house recommendation. The solid phase that also known as precursor was dry blended by hand mixing and shaking in a sealed bucket. The precursor was an aluminosilicate-rich naturally occurring rock normalized by active quenched blast furnace slag (BFS), an industrial waste, to achieve normalized chemical composition. In this study, the potassium silicate solution with a modular ratio of 2.49 was used as a hardener mixed with the precursors.

2.2 Molding, Curing, and Running Test. *Shear bond strength*—The shear bond strength test was performed by conducting the push-out test. The specimen consists of

(a) Inner pipe: A metal bar with a diameter of 51 mm and a height of 120 mm, which represents casing material.
(b) Outer pipe with an inner diameter of 150 mm: The outer pipe is functioned to hold the cementitious slurry during the curing period and as a casing material to measure the shear bond strength. Therefore, the shear bond strength for each sample of barrier material was measured twice; once, at the interface of a small bar with a diameter of 51 mm and next time, at the interface of the outer casing with an inner diameter of 150 mm.
(c) Stainless-steel bottom-cap: It has a hole with a diameter of 51.5 mm in the center to fix the metal bar. The bottom-cap also has a circular groove to hold the outer pipe. Plastic cellophane was placed on the bottom-cap to avoid any bonding between the slurry and the cap during the curing period. The bottom-cap was removed before running the shear bond strength rest.
(d) Stainless-steel top-cap: It is similar to the bottom-cap, but with two extra holes with a diameter of 20 mm, one for filling the cell and the other one for observing the level of liquid slurry inside the mold.

The whole system was assembled using silicon glue 1 day before mixing the slurry. The system was cured at 90 °C, corresponding to bottom-hole static temperature. However, the pressure for curing shear bond strength test specimens could not be increased above 500 psi due to safety issues and limitations with the curing chamber. After 7 days of curing, the samples were prepared for the push-out test to measure the shear bond strength test in short-term. The specimens were cooled down to the ambient temperature in 9 h to avoid thermal shock to the system. The bottom- and top-caps were removed slowly, and the samples were placed on a stand for applying loading rate. The stand was designed to only hold the cement sheath. Both the middle bar and outer pipe are free to move during loading. Initially, the bar was pushed until the bonding was broken. At this point, the bar started to move within the cement sheath. In the next step, the loading rate was applied to the outer pipe until it was debonded at the interface with the cement sheath. A universal testing machine (Zwick/Roell Z050) that is normally used for the compressive/tensile strength test was used as equipment to apply load on samples. Loading regime to push the bars and pipers may have an impact on the results, and it also depends on the sensitivity of the equipment. The equipment was programmed on load control mode rather than position control, and the loading rate of 50 N/s was selected. The reason for considering load control is presented in detail under Sec. 4. The whole process of sample preparation is illustrated graphically in Fig. 2.

Hydraulic bond strength—After mixing by API high-speed Waring blender, the barrier materials were transferred to the atmospheric consistometer and conditioned for 30 min at bottom-hole circulation temperature of 65 °C. The temperature controller was functioned to increase the temperature by 1 °C/min. After conditioning, the slurry was poured inside the casing pipes. The 120 mm casing pipe has an inner diameter of 37 mm and a thickness of 7 mm. Three holes are established at the center of the body with an orientation of 120 deg for pump connection and fluid injection. The pipes used for the hydraulic bond strength test were the same in composition and material as the solid bars used for the shear bond strength test. The samples were placed inside cylindrical autoclaves in the oven to be cured for 7 days. The temperature for curing was 90 °C, and a pump provided the pressure of 2500 psi in autoclaves. Three specimens were provided per barrier material with casing to minimize the possible errors in running the tests. After 7 days, the samples were cooled down slowly and connected to an ISCO pump for hydraulic testing and fluid injection. De-ionized water was used as an injection fluid. There is no common standard to evaluate the hydraulic bond strength of barrier materials for oil and gas applications. The pump was programmed to increase the pressure gradually in the following steps:

(1) From atmospheric to 100 psi in 1 min and hold at 100 psi for 10 min.
(2) From 100 to 150 psi in 1 min and hold at 150 psi for 10 min.
(3) From 150 to 200 psi in 1 min and hold at 200 psi for 5 min.

The neat class G cement was the first material to test the hydraulic bond strength. It was observed the samples start to lose their hydraulic sealability at 200 psi. It was not applicable to increase the differential pressure due to high fluid leak in specimens. However, the expansive cement and geopolymer showed no leakage and no sign of failure until 200 psi. Therefore, it was decided to increase the differential pressure up to 500 psi in following the steps:

(a) From 200 to 300 psi in 1 min and hold at 300 psi for 5 min.
(b) From 300 to 400 psi in 1 min and hold at 400 psi for 5 min.
(c) From 400 to 500 psi in 1 min and hold at 500 psi for 15 min.

The test stopped at 500 psi due to safety issues. Figure 3 graphically shows the setup for hydraulic bond strength. To avoid drying shrinkage, all testing samples for shear bond and hydraulic bond strength test were kept under water after removing the oven and running the experiments.

3 Experimental Results

3.1 Shear Bond Strength Test. The samples after 7-day curing were placed under compression load to run the push-out

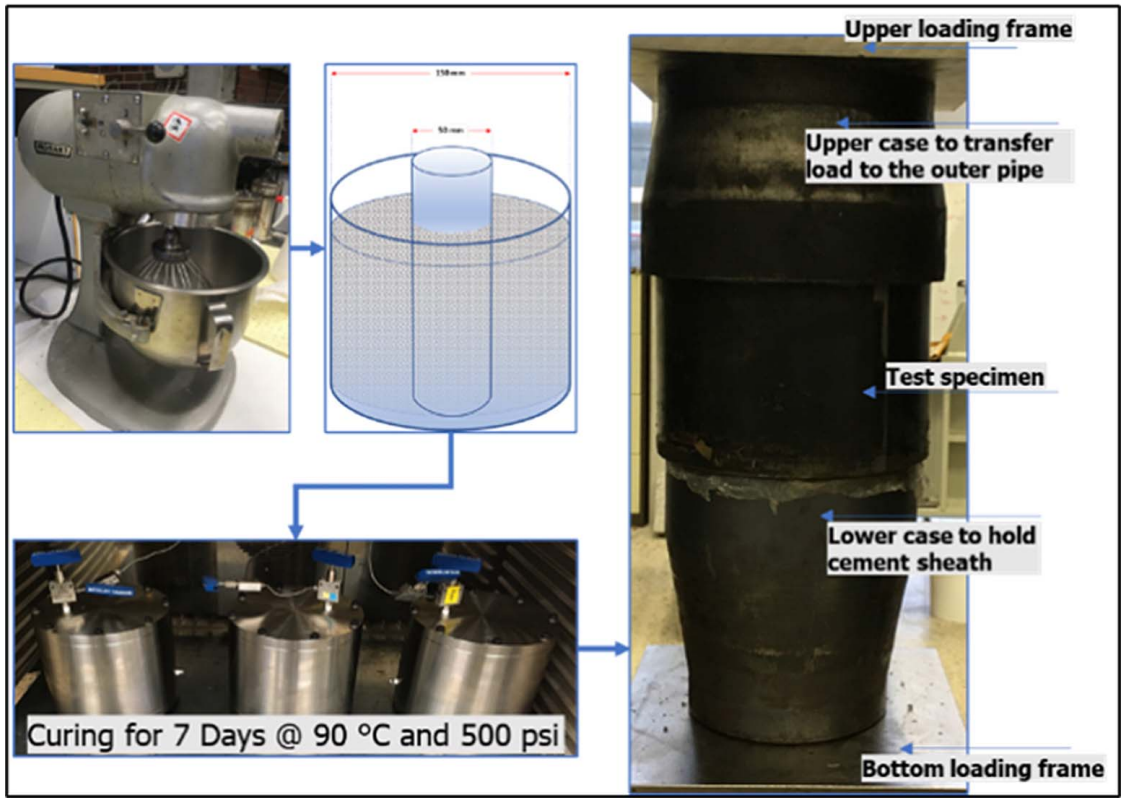

Fig. 2 The sample preparation process for the shear bond strength test, including mixing, molding, curing, and testing

Fig. 3 The sample preparation and test setup for the hydraulic bond strength test

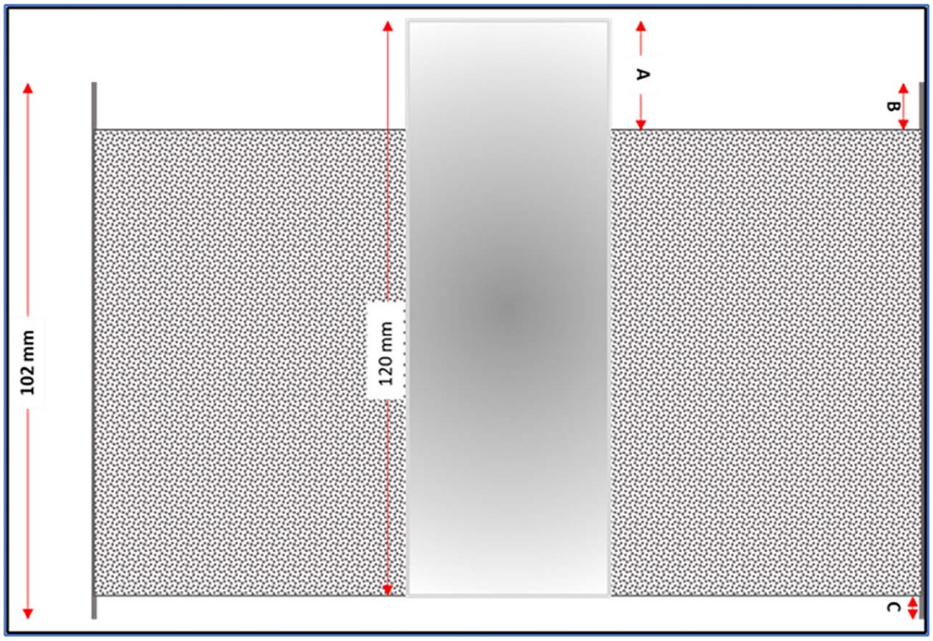

Fig. 4 The cross section of a shear bond strength test sample. A, B, and C should be measured for each specimen.

test. For every sample, the contact area of barrier material with the inner bar and the outer pipe was estimated before loading the specimen. The contact area was calculated by extracting A, B, and C for each sample as illustrated in Fig. 4.

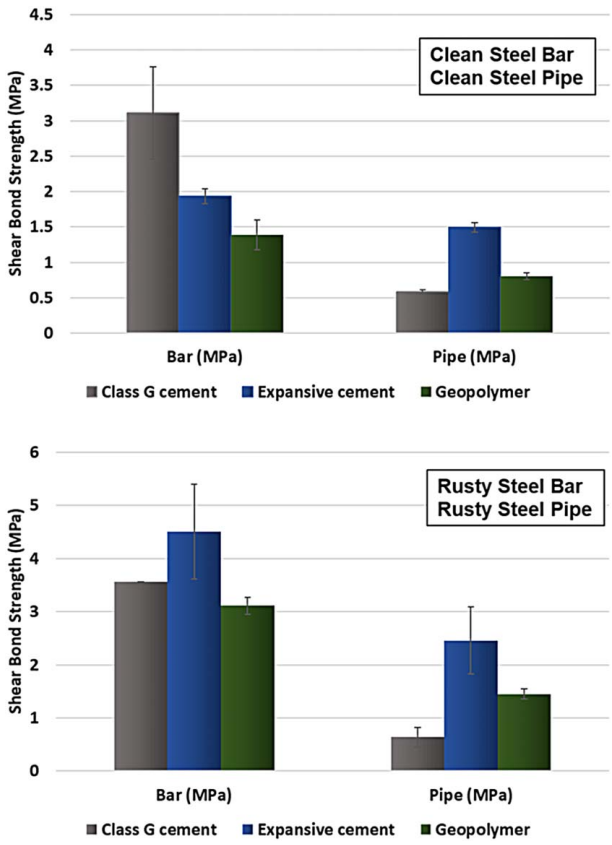

Fig. 5 Shear bond strength at the interface of solid bar and outer pipe for API neat class G cement, expansive cement, and geopolymer

Figure 5 shows the shear bond strength for the candidate barrier materials with both clean and rusty steels. The bond strength for all samples with rusty steel is increased. However, the bond strength of neat class G cement has less increase, by about 10% for both rusty bar and pipe steel compared with the clean steel surfaces. The reason for this lesser increase is not known. The shear bond strength of class G cement at the pipe interface was only 17% of the bond strength with the bar. In another study with the same cement and similar grade of steel bar in the middle, Khalifeh et al. [14] reported the shear bond strength of 1.3 MPa, which is 58% lower than the current measured strength. Following sample preparation procedure but increasing temperature by 20 °C and curing under elevated pressure of 3.4 MPa has positively impact shear bond strength.

The shear bond strength of expansive cement experienced about 100% increase when the rusty steel was considered, both at the pipe and bar interface. The shear bond strength at the bar interface was reached to the average value of 4.5 MPa, and at the pipe interface, the bond strength was measured 2.5 MPa, which is 55% of the bond strength at the bar interface.

The shear bond strength for the geopolymer was increased by 100% at both rusty bar and pipe interfaces. The shear bond strength of the geopolymer at the pipe surface was about 50% of strength at the bar interface for both clean and rusty boundaries.

The difference in shear bond strength of geopolymer and expansive cement with neat class G cement at outer pipe can be either related to the shrinkage of class G cement or chemical interactions between the barrier materials and surface minerals in the interface transition zone (ITZ). However, the chemical interaction between rust and different cementitious materials is not yet well understood.

3.2 Hydraulic Bond Strength Test. The hydraulic bond strength test goal was to qualitatively evaluate the hydraulic sealability at the interface of the barrier material and casing systems. The hydraulic bond strength test results for selected barrier materials and clean machined steel are shown in Fig. 6. The figure includes the flowrate (ml/min), cumulative injected fluid by the pump during the test period (ml) and pressure (psi). The neat class G cement–steel pipe system was considered as a reference in this study.

The high initial flowrate refers to the fluid to fill and pressurize the connected pipes to the samples, and it can be ignored. The

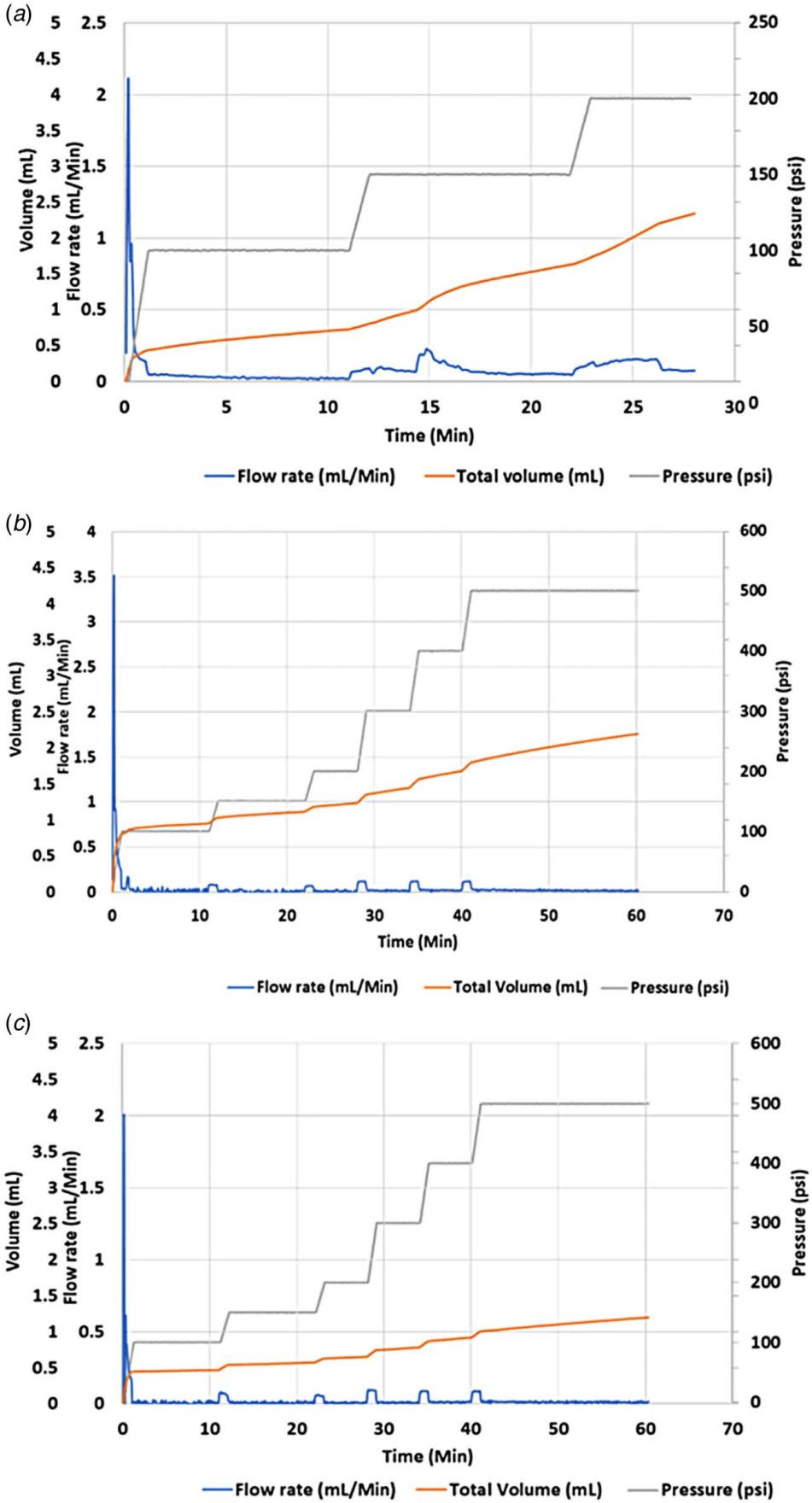

Fig. 6 Hydraulic bond strength test results for clean machined steel including the flowrate in ml/min, cumulative volume of injected fluid in ml, and pressure in psi for (*a*) API neat class G cement, (*b*) expansive cement, and (*c*) geopolymer

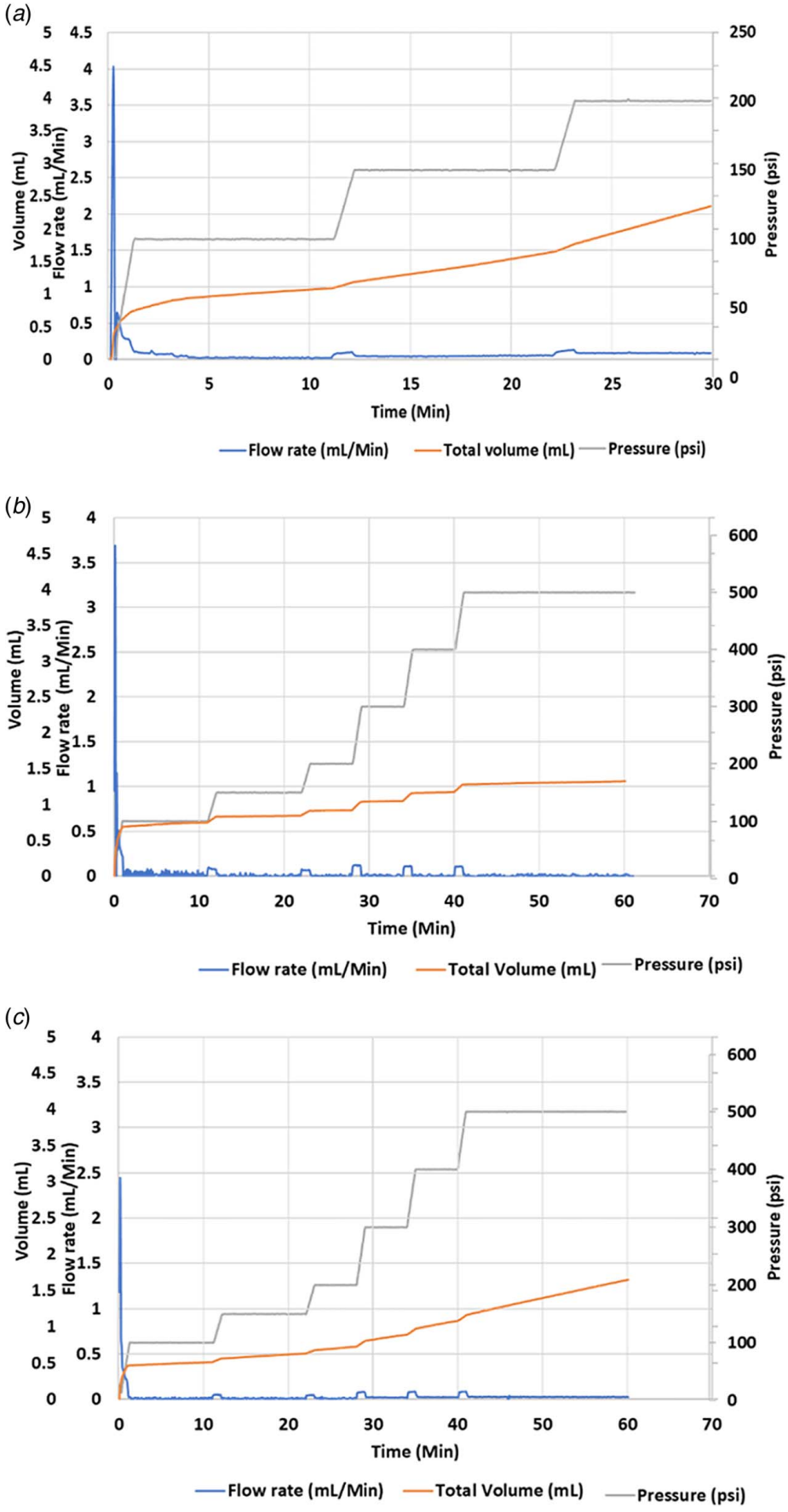

Fig. 7 Hydraulic bond strength test results for rusty steel including the flowrate in ml/min, cumulative volume of injected fluid in ml, and pressure in psi for (*a*) API neat class G cement, (*b*) expansive cement, and (c) geopolymer

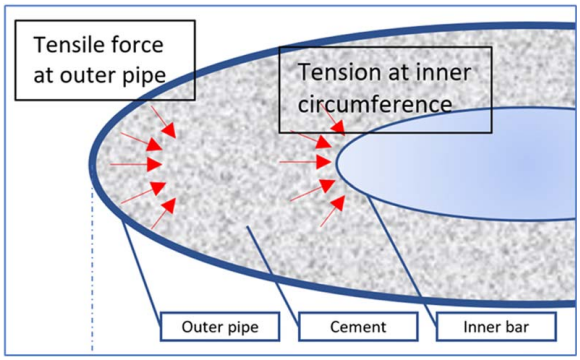

Fig. 8 Tensile loads due to cement shrinkage at outer and inner circumference of the cement sheath

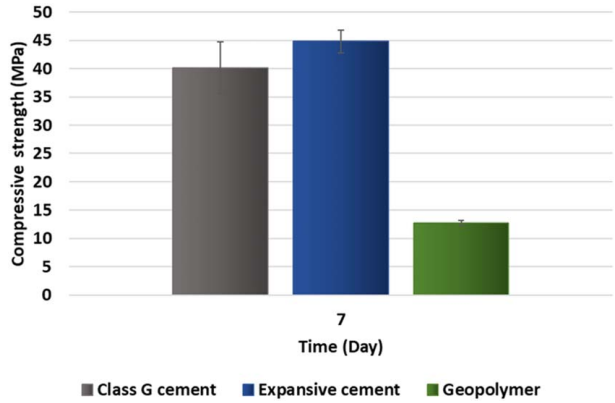

Fig. 9 Uniaxial compressive strength of barrier materials up to 7 days

small humps in the flowrate trend during the test are also referred to the increase in differential pressure. A relatively high flowrate was expected for the neat class G cement due to the autogenous shrinkage. The test was only continued up to differential pressure of 200 psi due to high leakage at the interfaces between pipe and cement and also cement matrix. Expansive cement and geopolymer could provide sealability up to 200 psi. The logged pump flowrate was negligibly low, compared with that of the neat class G cement (Fig. 6). Therefore, no fluid leak was observed at the interfaces and material matrices when the tests were continued up to 500 psi. Both expansive cement and geopolymer systems provided appropriate sealability comparing to the neat class G cement. The test results for the cementitious materials and rusty corroded steel are shown in Fig. 7. Similar to the clean steel test results, the samples followed almost the same trend. The geopolymer showed a minimum flowrate compared with the other systems. The hydraulic sealability of the expansive cement system was also in the same range of geopolymer.

4 Discussions

Shear bond strength—The shear bond strength of different barrier materials was measured at the inner and outer surfaces of the set barrier materials and steel. The shear bond strength test's main goal in the present work was predicting the pure shear force that is required to make a movement at the interface of the steel and barrier material by reducing the possible uncertainties. This is the main reason to consider a relatively thick sheath of barrier materials (about 50 mm) for molding and sample preparation. Thinner thicknesses could result in radial cracks due to the almost 70 °C difference between curing and testing temperatures. However, the samples were cooled down gradually for 9 h, but the difference in the thermal expansion coefficient of barrier materials and steel could cause radial cracks [27].

Additionally, the outer pipe was carbon steel grade S235JRH (roughness: 2.1, chemical composition: 2% carbon, 1.4% manganese, and 0% silicon), while the inner bar was chromium-rich grade 4140 (roughness: 2.07, chemical composition: 1.06% chromium, 0.91% manganese, 0.41% carbon, and 0.3% silicon). Suppose any possible chemical interaction affects bonding between the barrier material and the steel pipe. In that case, the chemical composition, and minerals at the surface of both barrier material and metal are the key parameters. Consequently, the effect of pipe diameter in the shear bond strength test is irrelevant in this study. Moreover, shrinkage due to the hydration reaction and chemistry of cement slurries is well-known. When the cement-based slurries are placed in a circular geometry, such as specimens that are provided for the shear bond strength test, cement shrinkage implies inward tension to the convex interface consisting of the interface between cement and middle bar. At the concave interface, the interface between cement and outer pipe, it is opposite. The interface of the cement and concave metal experiences a tension from the pipe-cement interface heading inward [27]. Figure 8 graphically illustrates the possible shrinkage tension regime that exists in a circular geometry. This can be an explanation for higher shear bond strength at the bar's interface (convex surface) compared with the outer pipe (concave surface).

Despite the shear bond strength test result reported by the previous literature, no fluctuation was observed in results after debonding occurred at the interface [11]. The loading mode applied by the equipment in the push-out test is an important parameter and may impact shear bond strength test results. The previous studies have selected position control to apply load on the samples. Generally, it is believed that for the compression tests of cementitious materials to measure uniaxial compressive strength, the control mode—position or load control—has no effect on stress–strain curves at the linear elastic range. In contrast, for the plastic range, the loading rate will be much lower than the load control, or the beginning of the position control [28]. By considering the displacement control mode selected by previous researchers for testing the samples, the fluctuation in the results may be due to the equipment adjustments to meet the selected testing mode. When the pipe starts to move within the cement sheath, dynamic friction exists at the interface of both materials. The equipment intends to meet the specified displacement rate; hence, it suddenly stops/reduces the loading rate on the sample. The dynamic friction coefficient changes to the static friction coefficient, which is greater than the dynamic one. Consequently, a more loading rate is required to push the pipe and reach the defined displacement rate, and the force starts to rise again. This oscillation behavior will repeat at entire time of the test after debonding occurs.

Evans and Carter found a correlation between compressive strength and shear bond strength of cement [10]. They showed a direct relationship between compressive strength and shear bond strength of the cement systems and stated that the supporting ability of cement could be determined if its compressive strength is available. The uniaxial compressive strength of the barrier materials was tested for up to 7 days of curing slurries under elevated temperature and pressure. The results are presented in Fig. 9 [26]. However, the mentioned relation between compressive strength and shear bond strength is only valid for the barrier materials and inner rusty bar. Still, for the outer pipe, the compressive strength was inversely proportional to the shear bond strength when geopolymer and cement systems are compared. Therefore, the correlation can be updated by including the different classes of barrier materials and the position of the casing pipe (inside or outside of the barrier material).

Hydraulic bond strength—Generally, as the curing condition is different from the testing conditions in the laboratory, the provided results cannot be extended to the real field application due to the

Fig. 10 Top: API neat class G samples started to leak both at interface and within the bulk at 100 psi of differential pressure. Middle: Expansive cement at 500 psi of differential pressure. Bottom: Geopolymer at 500 psi of differential pressure. Both expansive cement and geopolymer revealed no fluid leakage within the bulk.

uncertainties. Therefore, it is recommended to consider the results to make only a qualitative comparison between different casing materials and cementitious barrier materials.

The curing condition, samples preparation, casing material, and the casing inside diameter were the same for different cementitious materials. Hence, any difference in hydraulic sealability can be divided into two sections:

(1) At the casing-barrier material's interface, either by possible constructive reactions between the components of the set barrier material and the casing to form a tight and integrated sealing at the interfaces, and shrinkage compensation of the cementitious material. The neat class G cement is expected to experience an autogenous shrinkage due to the hydration reaction, which applies extra tension at the interfaces. The

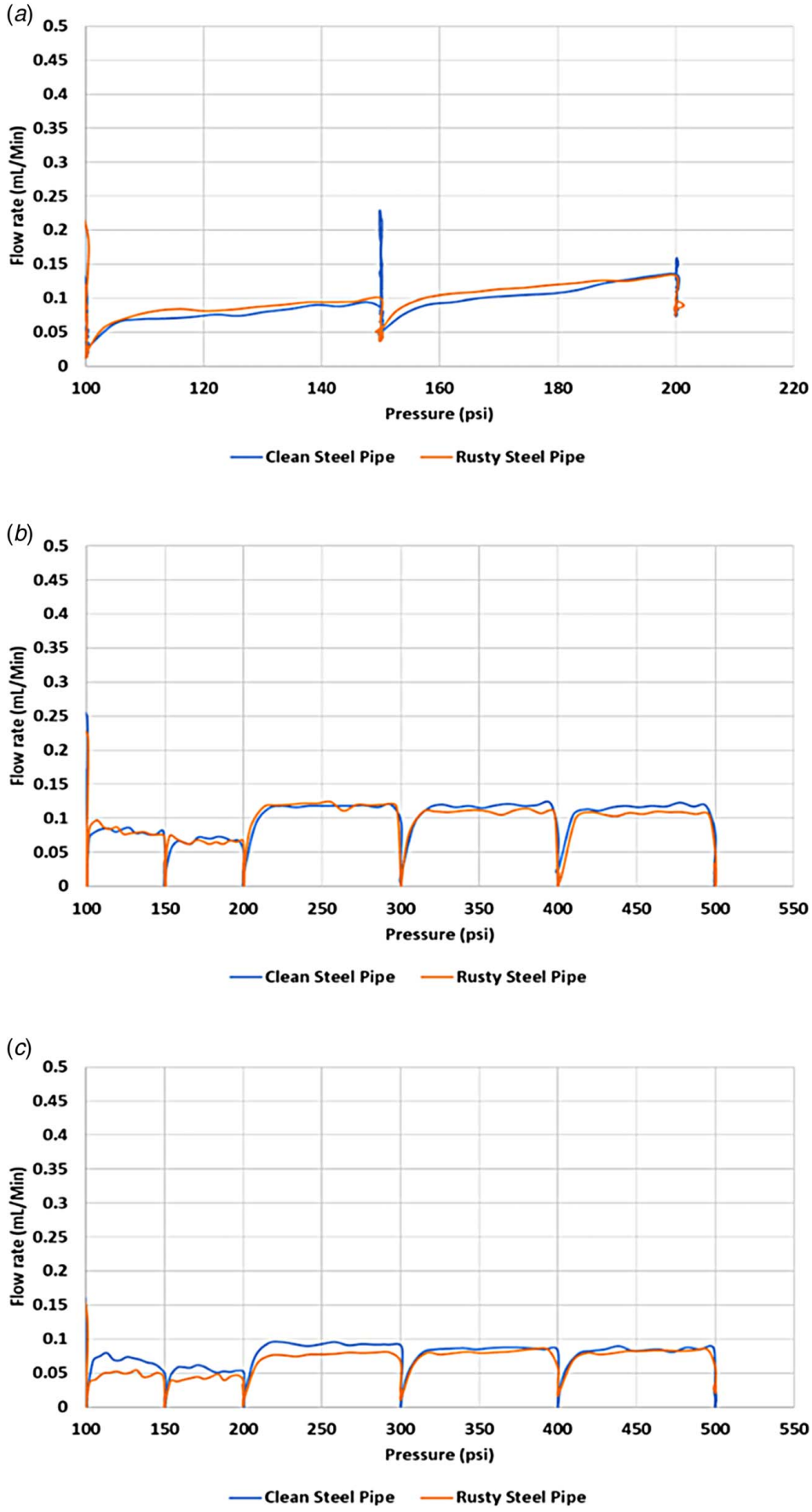

Fig. 11 The injection flowrate as function of differential pressure for clean steel pipe and rusty steel pipe for (*a*) API neat class G cement, (*b*) expansive cement, and (*c*) geopolymer

role of chemical additive and expansive agent in the expansive cement was brilliant in the test results. Although the geopolymer slurry follows a different reaction path for solidification, similar chemical components responsible for shrinkage compensation in expansive cement exist in geopolymer slurry. The BFS used in the geopolymer precursor significantly contributes to both shear and hydraulic bond strengths. The slag can develop internal stresses caused by densified microstructure. This feature can later result in rebonding and healing performance at the interface [29].

(2) Within the matrix of the barrier material. During the hydraulic bond strength test for the neat class G cement, it was observed that the injected fluid not only leaked at the cement–casing interface but also found its way through the cement matrix due to higher permeability comparing to expansive cement and geopolymer. Figure 10 clearly shows the fluid penetration and at the API net class G's surface. Accordingly, the additives used in expansive cement and the chemical composition of geopolymer improved the hydraulic sealing capability by providing a less permeable structure for the materials.

Except for the neat class G cement system, the results from rusty steel pipes comparing to the clean steel pipes showed that the rusted steel had provided a slightly better sealing capability for the same barrier material, as presented in Fig. 11. This observation may reveal that the rough surface at the interface can disconnect possible macro paths or more meandrous micro paths, which take for time for the fluid to move at the interface. A similar observation was reported by other researchers [30]. Running CFD analysis and X-ray CT techniques can help to understand the micro annular path's direction and size.

5 Conclusion

Two alternative barrier materials, including expansive cement and geopolymer, were highlighted, and shear bond and hydraulic bond strengths were tested. The neat API class G cement was also selected as a noncommercial reference. The shear bond strength of barrier materials and steel casing summarizes different parameters such as surface geometry, chemical and mechanical characteristics of both barrier material and casing. The mineralogy of materials at the contact interface can influence the bonding in the short- and long-term. Therefore, the interface transition zone of the barrier material and metal should be studied in detail. The strong shear bond strength may not be representative of good zonal isolation individually; hence, the mechanical properties of the materials, such as compressive and tensile strengths and modulus of flexibility, should also be included to evaluate the performance of the whole system.

The hydraulic sealability of the zonal isolation materials with clean and rusty steel was tested by continuously injecting water at the barrier material-casing interface. Both expansive cement and geopolymer showed sealing capability during the test period and up to 0.34 MPa (500 psi) of differential pressure. The injection flowrate can be considered as a function of possible micro annular paths at the interfaces. The rusty steel pipes showed slightly better hydraulic sealability, which can be due to the tortuous flow path formation. The chemical interaction between cement and rusty steel or clean steel at the interface transition zone remains a question. The difference in curing condition of pressure and temperature with the testing condition at room temperature and pressure is non-negligible; thus, further studies are required to extend the field application results.

Acknowledgment

The authors would like to thank Halliburton and AlTiSS AS for their supports and for sharing technical information. A special thanks go to Johannes Steinnes Jensen and Emin Ahmadov for preparing the test setup for curing samples. The authors also thank Aker BP and TOTAL for supporting part of the project through the SafeRock Project joint industrial project at the University of Stavanger (UiS).

Conflict of Interest

There are no conflicts of interest.

Data Availability Statement

The datasets generated and supporting the findings of this article are obtainable from the corresponding author upon reasonable request. The authors attest that all data for this study are included in the paper. Data provided by a third party are listed in Acknowledgment.

Funding Data

- Research Council of Norway (KD) through the Department of Energy and Petroleum Engineering (IEP), University of Stavanger (UiS).

References

[1] Vrålstad, T., Saasen, A., Fjær, E., Øia, T., Ytrehus, J. D., and Khalifeh, M., 2019, "Plug & Abandonment of Offshore Wells: Ensuring Long-Term Well Integrity and Cost-Efficiency," J. Pet. Sci. Eng., **173**, pp. 478–491.

[2] Alvi, M. A. A., Khalifeh, M., and Agonafir, M. B., 2020, "Effect of Nanoparticles on Properties of Geopolymers Designed for Well Cementing Applications," J. Pet. Sci. Eng., **191**, pp. 107–128.

[3] Opedal, N., Todorovic, J., Torsaeter, M., Vralstad, T., and Mushtaq, W., 2014, "Experimental Study on the Cement-Formation Bonding," SPE International Symposium and Exhibition on Formation Damage Control, Lafayette, LA, February, Society of Petroleum Engineers.

[4] Skadsem, H. J., and Kragset, S., 2021, "Effect of Buoyancy and Inertia on Viscoplastic Fluid–Fluid Displacements in a Regular and an Irregular Eccentric Annulus," ASME J. Energy Resour. Technol., **143**(6), p. 062101.

[5] Jafariesfad, N., Geiker, M. R., Gong, Y., Skalle, P., Zhang, Z., and He, J., 2017, "Cement Sheath Modification Using Nanomaterials for Long-Term Zonal Isolation of Oil Wells," J. Pet. Sci. Eng., **156**, pp. 662–672.

[6] Kimanzi, R., Wu, Y., Salehi, S., Mokhtari, M., and Khalifeh, M., 2020, "Experimental Evaluation of Geopolymer, Nano-Modified, and Neat Class H Cement by Using Diametrically Compressive Tests," ASME J. Energy Resour. Technol., **142**(9), p. 092101.

[7] Khalifeh, M., Saasen, A., Hodne, H., Godøy, R., and Vrålstad, T., 2018, "Geopolymers as an Alternative for Oil Well Cementing Applications: A Review of Advantages and Concerns," ASME J. Energy Resour. Technol., **140**(9), p. 092801.

[8] Khalifeh, M., and Saasen, A., 2020, *Introduction to Permanent Plug and Abandonment of Wells*, Springer Nature, The Hague.

[9] Opedal, N., Cerasi, P., and Vrålstad, T., 2019, "Cement Bond Strength Measurements," International Conference on Offshore Mechanics and Arctic Engineering, Glasgow, Scotland, UK, November, American Society of Mechanical Engineers.

[10] Evans, G. W., and Carter, L. G., 1962, "Bounding Studies of Cementing Compositions to Pipe and Formations," Presented at the Drilling and Production Practice, New York, January, American Petroleum Institute.

[11] Kakumoto, M., Yoneda, J., Tenma, N., Miyazaki, K., Aoki, K., and Itoi, R., 2012, "Frictional Strength Between Casing and Cement Under Confining Pressure," The Twenty-Second International Offshore and Polar Engineering Conference, Rhodes, Greece, June, International Society of Offshore and Polar Engineers.

[12] Lavrov, A., Bhuiyan, M., and Stroisz, A., 2019, "Push-Out Test: Why Bother?" J. Pet. Sci. Eng., **172**, pp. 297–302.

[13] Lavrov, A., Gawel, K., Stroisz, A., Torsæter, M., and Bakheim, S., 2017, "Failure Modes in Three-Point Bending Tests of Cement-Steel, Cement-Cement and Cement-Sandstone Bi-Material Beams," Constr. Build. Mater., **152**, pp. 880–886.

[14] Khalifeh, M., Hodne, H., Saasen, A., Dziekonski, M., and Brown, C., 2018, "Bond Strength Between Different Casing Materials and Cement," SPE Norway One Day Seminar, Bergen, Norway, April, Society of Petroleum Engineers.

[15] Zhang, H. Y., Kodur, V., Qi, S. L., and Wu, B., 2015, "Characterizing the Bond Strength of Geopolymers at Ambient and Elevated Temperatures," Cem. Concr. Compos., **58**, pp. 40–49.

[16] Salehi, S., Khattak, M. J., and Bwala, A. H., 2017, "Characterization, Morphology and Shear Bond Strength Analysis of Geopolymers: Implications for Oil and Gas Well Cementing Applications," J. Nat. Gas Sci. Eng., **38**, pp. 323–332.

[17] Khalifeh, M., Saasen, A., Hodne, H., and Motra, H. B., 2019, "Laboratory Evaluation of Rock-Based Geopolymers for Zonal Isolation and Permanent P&A Applications," J. Pet. Sci. Eng., **175**, pp. 352–362.
[18] Ytrehus, J. D., Lund, B., Taghipour, A., Kosberg, B. R., Carazza, L., Gyland, K. R., and Saasen, A., 2021, "Hydraulic Behavior in Cased and Open-Hole Sections in Highly Deviated Wellbores," ASME J. Energy Resour. Technol., **143**(3), p. 033008.
[19] Bybee, K., 2005, "The Cement-to-Formation Interface in Zonal Isolation," J. Pet. Technol., **57**(08), pp. 41–44.
[20] Lecampion, B., Bunger, A., Kear, J., and Quesada, D., 2013, "Interface Debonding Driven by Fluid Injection in a Cased and Cemented Wellbore: Modeling and Experiments," Int. J. Greenhouse Gas Control, **18**, pp. 208–223.
[21] De Andrade, J., Sangesland, S., Skorpa, R., Todorovic, J., and Vrålstad, T., 2016, "Experimental Laboratory Setup for Visualization and Quantification of Cement-Sheath Integrity," SPE Drill. Eng., **31**(04), pp. 317–326.
[22] Henkensiefken, R., Bentz, D., Nantung, T., and Weiss, J., 2009, "Volume Change and Cracking in Internally Cured Mixtures Made With Saturated Lightweight Aggregate Under Sealed and Unsealed Conditions," Cem. Concr. Compos., **31**(7), pp. 427–437.
[23] Nagelhout, A., Bosma, M. G., Mul, P., Krol, G., van Velzen, H., Joldersma, J., James, S. G., Dargaud, B., Schreuder, R., and Théry, F., 2010, "Laboratory and Field Validation of a Sealant System for Critical Plug-and-Abandon Applications," SPE Drill. Eng., **25**(03), pp. 314–321.
[24] Thomas, J., Musso, S., Catheline, S., Chougnet-Sirapian, A., and Allouche, M., 2014, "Expanding Cement for Improved Wellbore Sealing: Prestress Development, Physical Properties, and Logging Response," SPE Deepwater Drilling and Completions Conference, Galveston, TX, September, Society of Petroleum Engineers.
[25] Salehi, S., Khattak, M. J., Ali, N., Ezeakacha, C., and Saleh, F. K., 2018, "Study and Use of Geopolymer Mixtures for Oil and Gas Well Cementing Applications," ASME J. Energy Resour. Technol., **140**(1), p. 012908.
[26] Kamali, M., Khalifeh, M., Saasen, A., Godøy, R., and Delabroy, L., 2021, "Alternative Setting Materials for Primary Cementing and Zonal Isolation—Laboratory Evaluation of Rheological and Mechanical Properties," J. Pet. Sci. Eng., **201**, p. 108455.
[27] Torsæter, M., Todorovic, J., and Lavrov, A., 2015, "Structure and Debonding at Cement–Steel and Cement–Rock Interfaces: Effect of Geometry and Materials," Constr. Build. Mater., **96**, pp. 164–171.
[28] American Petroleum Institute, 2017, *API TR 10TR7, Mechanical Behavior of Cement*, API, Washington, DC.
[29] Blanco, A., Colina, A., Rodriguez, W., and Bolivar, R., 1999, "Effective Pay Zone Isolation of Steam Injection Wells," Latin American and Caribbean Petroleum Engineering Conference, Caracas, Venezuela, April, Society of Petroleum Engineers.
[30] Corina, A. N., Skorpa, R., Sangesland, S., and Vrålstad, T., 2020, "Simulation of Fluid Flow Through Real Microannuli Geometries," J. Pet. Sci. Eng., **196**, p. 107669.